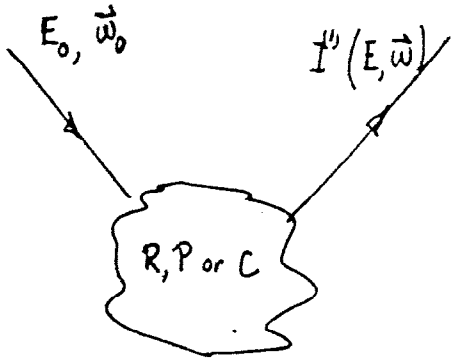

Single interaction process

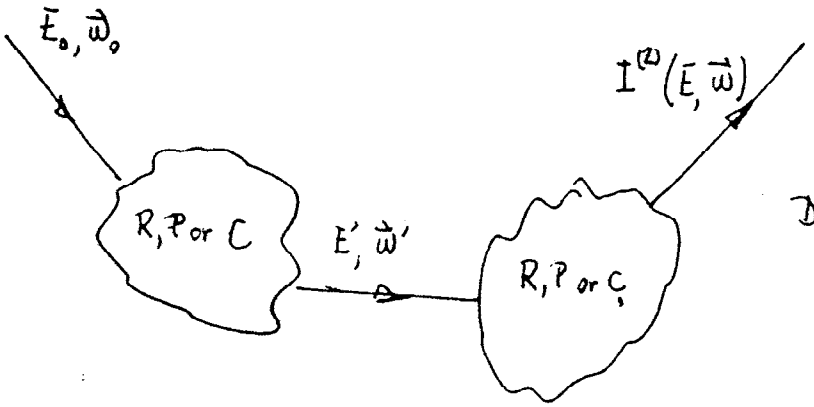

Double interaction process

a \ b	Photoelectric effect	Coherent (Rayleigh) scattering	Incoherent (Compton) scattering
Photo-electric effect	Secondary XRF intensity[1]	XRF intensity scattered from other scatter centers to the detector[3]	Modification of the symmetry of the XRF line due to the lower energy Compton emiss.[3]
Coherent (Rayleigh) scattering	Coherent scattering enhancement to the XRF intensity[2]	Double scattering Rayleigh[4]	Double scattering Compton (this work)
Incoherent (Compton) scattering	Incoherent scattering enhancement to the XRF intensity[2]	Double scattering Rayleigh-Compton (this work)	Double scattering Compton-Rayleigh (this work)

Physical meaning of every chain of interactions (a, b) for the main processes affecting soft X-rays.

First order interaction

PHOTOELECTRIC

$$I_p^{(1)}(\vec{\omega},\lambda) = \frac{I_0}{4\pi} \frac{1+\cos^2\theta}{2} \frac{1-\cos\theta}{2} \sum_i \frac{|\gamma|}{\mu(\lambda)|\rho| + \mu_0|\gamma|}$$

$$\delta(\lambda-\lambda_i)\, Q_{\lambda_i}(\lambda_0)\left[1-U(\lambda_0-\lambda_{ei})\right]$$

RAYLEIGH

$$I_R^{(1)}(\vec{\omega},\lambda) = I_0 \frac{1+\cos^2\theta}{2} \frac{1-\cos\theta}{2} \frac{|\gamma|}{\mu(\lambda)|\rho| + \mu_0|\gamma|}$$

$$S(\lambda-\lambda_0)\,\sigma\left[1+(\vec{\omega}\cdot\vec{\omega}_0)^2\right] \frac{F^2(\lambda_0, \vec{\omega}\,\vec{\omega}_0, Z)}{Z} \qquad \sigma = \frac{\rho N Z}{A} r_e^2$$

COMPTON

$$I_C^{(1)}(\vec{\omega},\lambda) = I_0 \frac{1+\cos^2\theta}{2} \frac{1-\cos\theta}{2} \frac{|\gamma|}{\mu(\lambda)|\rho| + \mu_0|\gamma|}$$

$$\sigma\, K_{KN}(\lambda,\lambda_0)\, S(\lambda_0, \vec{\omega}\cdot\vec{\omega}_0, Z)\, \delta\left((1-\vec{\omega}_0\cdot\vec{\omega})\lambda_c + \lambda_0 - \lambda\right)$$

SOME PROPERTIES OF THE FIRST ORDER INTERACTIONS

PHOTOELECTRIC

- Azimuthal symmetry
- Discrete at $\lambda = \lambda_i$ $(i = 1, \dots, N)$
- Every line with different intensity given by $Q_{1i}(\lambda_0)$ and by the absorption

RAYLEIGH

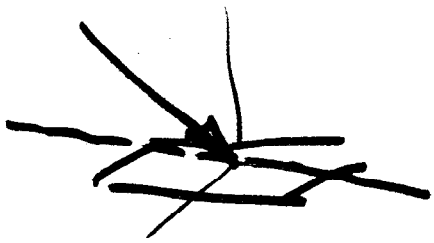

- Plane of symmetry (not an axis)
- Discrete at $\lambda = \lambda_0$

COMPTON

- Plane of symmetry
- Discrete at $\lambda = \lambda_0 + \underbrace{\lambda_c (1 - \vec{\omega} \cdot \vec{\omega}_0)}_{\Delta\lambda}$

MANY ELEMENTS

- We assume isolated atoms

Mass absorption coefficient

$$\frac{\mu}{\rho} = \sum_j W_j \left(\frac{\mu}{\rho}\right)_j$$

W_j: weight fraction of element j in the mixture

$\left(\frac{\mu}{\rho}\right)_j$: mass absorption coefficient of element j

$$\frac{\mu}{\rho}\left[\frac{cm^2}{g}\right] = N_0 \frac{NZ}{A}$$

N_0: barn/electron

$$\mu[cm^{-1}] = \rho\left(\frac{\mu}{\rho}\right)$$

To get the composition dependence we must change from attenuation coefficients in $[cm^{-1}]$ to mass attenuation coeff in $[cm^2/g]$

$$I_p''(\bar{\omega}, \lambda) = \frac{I_0}{4\pi} \frac{|T|}{\mu|T_0| + \mu_0|T|} \sum_i \delta(\lambda - \lambda_i) Q_{\lambda_i}(t_0)$$

$$= \frac{I_0}{4\pi} \frac{|T|}{\sum_j \left[\left(\frac{\mu_0}{\rho}\right)_j |T_0| + \left(\frac{\mu}{\rho}\right)_j |T|\right] W_j} \sum_i \delta(\lambda - \lambda_i) Q_{\lambda_i}(t_0)$$

has the factor $\left(\frac{\tau}{\rho}\right)_i W_i$

It is possible to write the following set of equations

$$\frac{4\pi}{\lambda} \frac{I_p^{(1)}(\vec{\alpha},\lambda)}{I_0} \sum_j W_j \left[\left(\frac{\mu_i}{\rho}\right)_j \rho_0 l + \left(\frac{\mu_i}{\rho}\right)_j \rho_1 l \right] = \underbrace{Q_{ij}^*(\lambda)}_{\text{for } W_j = 1} W_j$$

for as many lines as elements we get

$$\Pi \vec{W} = Q \vec{W}$$

and with the constraint

$$\sum_j W_j = 1$$

XRF INTENSITIES

$$I^{(1)}(0,\vec{\omega},\lambda) = \frac{I_0}{4\pi}\,\frac{(1+\operatorname{sgn}\eta_0)}{2}\,\frac{(1-\operatorname{sgn}\eta)}{2}\,\frac{|\eta|}{\mu\,|\eta_0|+\mu_0|\eta|}\,\times$$

$$\sum_i \delta(\lambda-\lambda_i)\; Q_{\lambda_i}(\lambda_0)\left[1-U(\lambda_0-\lambda_{e_i})\right]$$

$$I^{(2)}(0,\vec{\omega},\lambda) = \frac{I_0}{4\pi}\,\frac{(1+\operatorname{sgn}\eta_0)}{2}\,\frac{(1-\operatorname{sgn}\eta)}{2}\,\frac{|\eta|}{\mu\,|\eta_0|+\mu_0|\eta|}\,\times$$

$$\sum_i \delta(\lambda-\lambda_i)\sum_j \frac{Q_{\lambda_j}(\lambda_0)\,Q_{\lambda_i}(\lambda_j)}{2}\left[1-U(\lambda_0-\lambda_{e_j})\right]\left[1-U(\lambda_j-\lambda_{e_i})\right]\times$$

$$\left\{\frac{|\eta_0|}{\mu_0}\,\ell n\left(1+\frac{\mu_0}{\mu_j|\eta_0|}\right)+\frac{|\eta|}{\mu}\,\ell n\left(1+\frac{\mu}{\mu_j|\eta|}\right)\right\}$$

$$I^{(3)}(0,\vec{\omega},\lambda) = \frac{I_0}{4\pi}\,\frac{(1+\operatorname{sgn}\eta_0)}{2}\,\frac{(1-\operatorname{sgn}\eta)}{2}\,\frac{|\eta|}{\mu\,|\eta_0|+\mu_0|\eta|}\,\times$$

$$\sum_i \delta(\lambda-\lambda_i)\sum_j\sum_k \frac{Q_{\lambda_k}(\lambda_0)\,Q_{\lambda_j}(\lambda_k)\,Q_{\lambda_i}(\lambda_j)}{4}\,\times$$

$$\left[1-U(\lambda_0-\lambda_{e_k})\right]\left[1-U(\lambda_k-\lambda_{e_j})\right]\left[1-U(\lambda_j-\lambda_{e_i})\right]\times$$

$$\left\{\frac{|\eta_0|}{\mu_0}\,\ell n\left(1+\frac{\mu_0}{\mu_k|\eta_0|}\right)\left\{\frac{|\eta_0|}{\mu_0}\,\ell n\left(1+\frac{\mu_0}{\mu_j|\eta_0|}\right)+\frac{|\eta|}{\mu}\,\ell n\left(1+\frac{\mu}{\mu_j|\eta|}\right)\right\}+\right.$$

$$\frac{\eta^2}{\mu^2}\,\ell n\left(1+\frac{\mu}{\mu_k|\eta|}\right)\ell n\left(1+\frac{\mu}{\mu_j|\eta|}\right)+$$

$$\left.\frac{1}{\mu_k}\int_0^{\mu_k/\mu_j}\frac{ds}{\frac{\mu_k}{s}+\frac{\mu_0}{|\eta_0|}}\,\ell n\left(\frac{1+s}{s}\right)+\frac{1}{\mu_j}\int_0^{\mu_j/\mu_k}\frac{ds}{\frac{\mu_j}{s}+\frac{\mu}{|\eta|}}\,\ell n\left(\frac{1+s}{s}\right)\right\}$$

- gives a shorter tertiary expression but also the new integrals have a more stable numerical behavior for $\mu_0 < 1$ (as may occur with high excitation energies).

- the possibility of having line enhancement in a pure target is signaled (since photons are bosons they do not follow an exclusion principle).
  By example, the L lines of a pure element (of medium or high atomic number) suffer the enhancement of its own K lines.

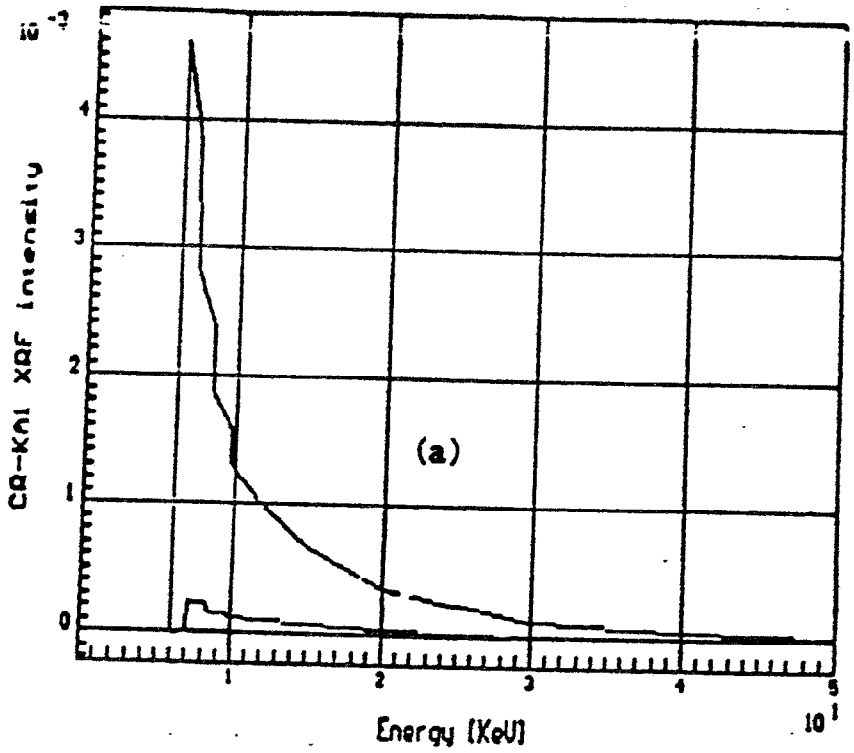

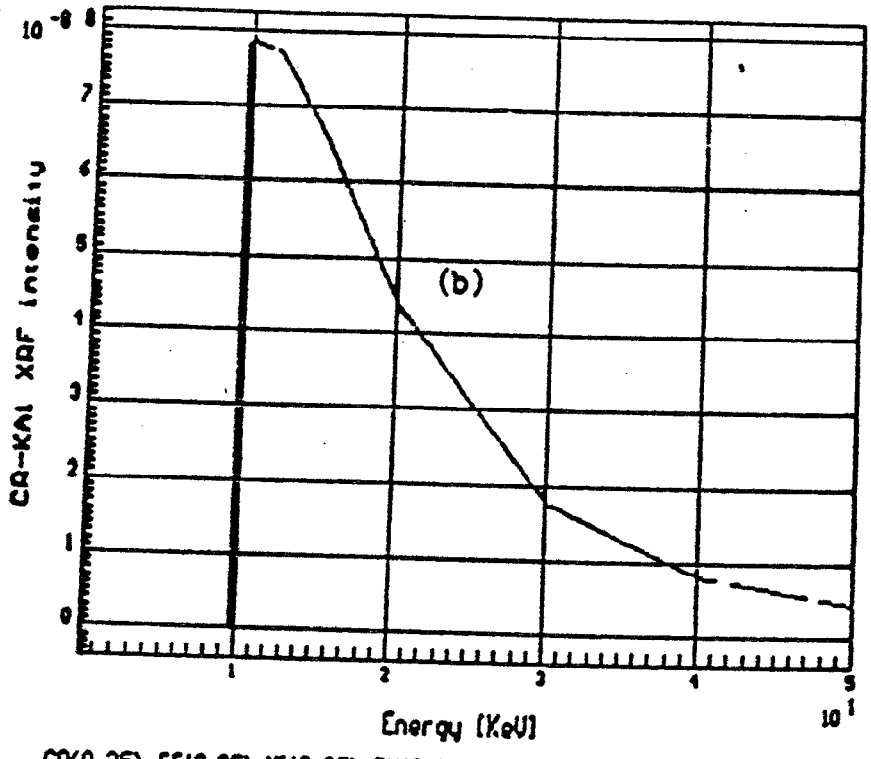

A graphical comparison of the different orders of enhancement for a single chain of $K\alpha_1$ lines. The sample is Zn(25 %)-Ni(25 %)-Fe(25 %)-Cr(25 %) and the geometry is fixed. (a) All the orders are plotted in the same graphic to compare them. (b) The fourth order is plotted separately.

EXAMPLE

Determine the composition of a Steel Fe-Ni that has the following spectrum of emission

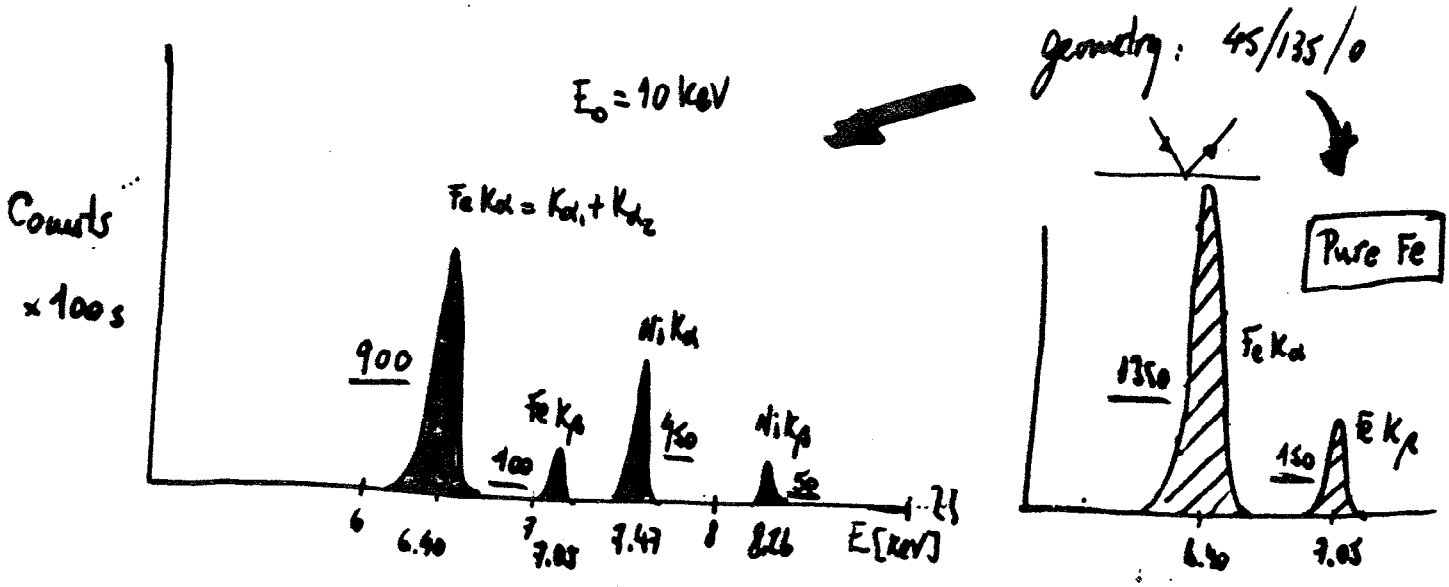

Data

Fe (Z = 26)

$\left(\frac{\mu}{\rho}\right)_{Fe}(10\ keV) = 172.86$

$\left(\frac{\tau}{\rho}\right)_{Fe}(10\ keV) = 171.51$

$\left(\frac{\mu}{\rho}\right)_{Fe}(6.40) = 70.46$

$\left(\frac{\mu}{\rho}\right)_{Fe}(7.05) = 53.48$

$\left(\frac{\mu}{\rho}\right)_{Fe}(7.47) = 303.07$

$\left(\frac{\mu}{\rho}\right)_{Fe}(8.26) = 284.27$

$I_{K\alpha} : I_{K\beta} = 9:1$

$r_k = 8.33$

$\omega_k = 0.338$

Ni (Z = 28)

$\left(\frac{\mu}{\rho}\right)_{Ni}(10\ keV) = 210.79$

$\left(\frac{\tau}{\rho}\right)_{Ni}(10\ keV) = 209.23$

$\left(\frac{\mu}{\rho}\right)_{Ni}(6.40) = 91.89$

$\left(\frac{\mu}{\rho}\right)_{Ni}(7.05) = 70.33$

$\left(\frac{\mu}{\rho}\right)_{Ni}(7.47) = 59.91$

$\left(\frac{\mu}{\rho}\right)_{Ni}(8.26) = 45.33$

$I_{K\alpha} : I_{K\beta} = 9:1$

$r_k = 7.85$

$\omega_k = 0.414$

We assume that $I(\vec{w},1) = I^{(1)}(\vec{w},1)$

and select Fe K_α that we have in both spectra (unknown sample and pure Fe)

We do the ratio $\frac{I_{Fe\text{-}unknown}}{I_{Fe\text{-}pure}}$ to factor out I_0 (that is unknown)

$$R = \frac{I_{Fe-u}}{I_{Fe-p}} = \frac{Q^*_{Fe}(10\,keV)\, W_{Fe}}{\sum_j \left[\left(\frac{\mu}{\rho}\right)_j (6.40\,keV) + \left(\frac{\mu}{\rho}\right)_j (10\,keV)\right] W_j} \cdot \frac{\left(\frac{\mu}{\rho}\right)_{Fe}(6.40\,keV) + \left(\frac{\mu}{\rho}\right)_{Fe}(10\,keV)}{Q^*_{Fe}(10\,keV)}$$

$$\Rightarrow (R-1)\, W_{Fe} + R\left[\frac{\left(\frac{\mu}{\rho}\right)_{Ni}(6.40) + \left(\frac{\mu}{\rho}\right)_{Ni}(10)}{\left(\frac{\mu}{\rho}\right)_{Fe}(6.40) + \left(\frac{\mu}{\rho}\right)_{Fe}(10)}\right] W_{Ni} = 0 \qquad (E.1)$$

We have the additional equation

$$W_{Fe} + W_{Ni} = 1 \qquad (E.2)$$

From (E.1) and (E.2) we get the composition.

$$\begin{aligned} -0.33\, W_{Fe} + 0.829\, W_{Ni} &= 0 \\ W_{Fe} + W_{Ni} &= 1 \\ \sim\sim\sim\sim\sim\sim\sim\sim \\ W_{Fe} - 2.51\, W_{Ni} &= 0 \\ - \quad W_{Fe} + W_{Ni} &= 1 \\ \hline -3.51\, W_{Ni} &= -1 \end{aligned}$$

$\Rightarrow$ $W_{Ni} = 0.285$

$W_{Fe} = 1 - W_{Ni} = 0.715$

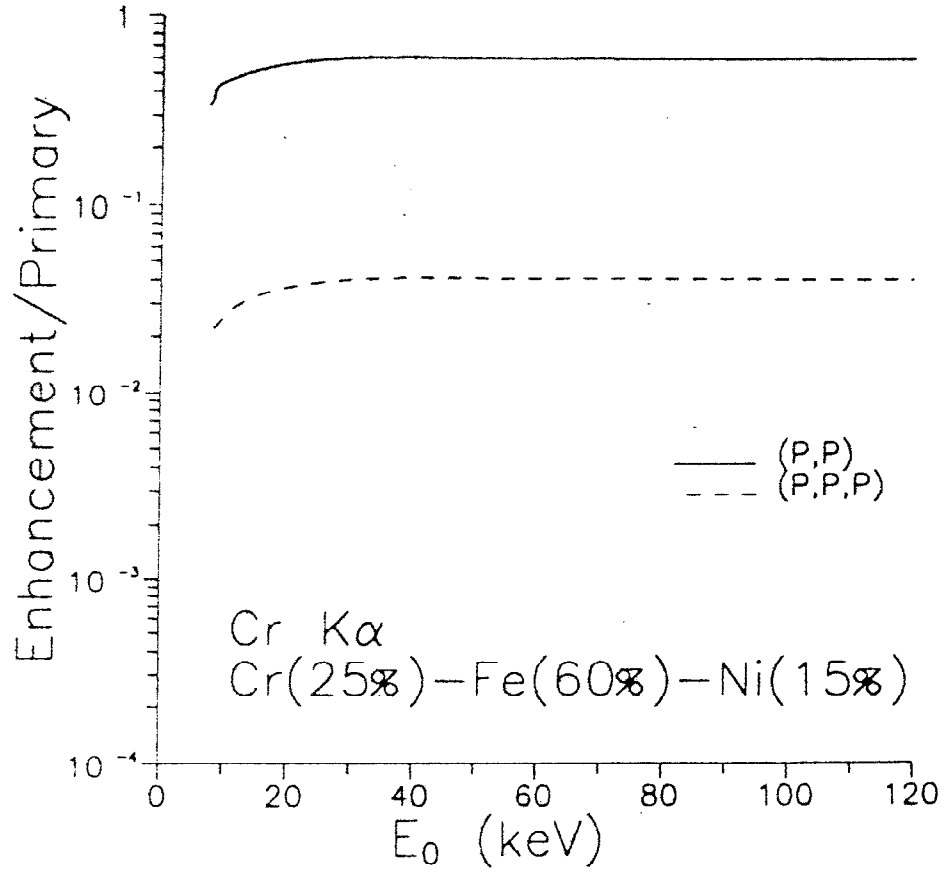
Enhancement/Primary
1
10^{-1}
10^{-2}
10^{-3}
10^{-4}
(P,P)
(P,P,P)
Cr Kα
Cr(25%)–Fe(60%)–Ni(15%)
0
20
40
60
80
100
120
E_0 (keV)

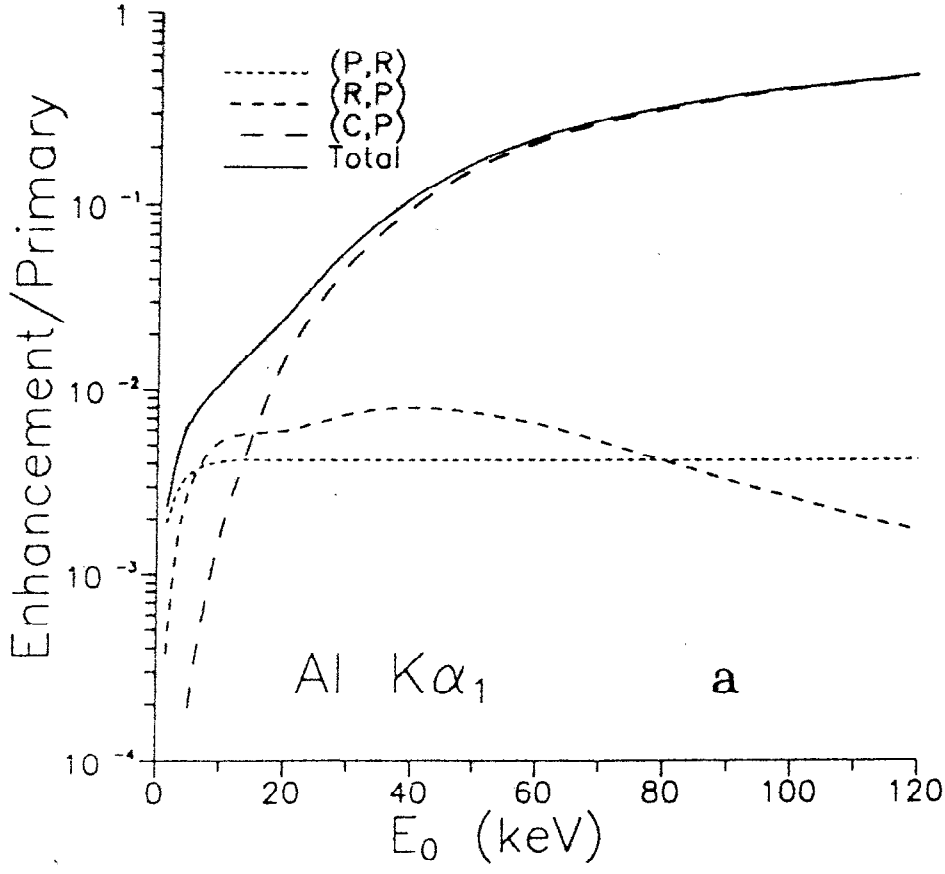
Enhancement/Primary
1
10^{-1}
10^{-2}
10^{-3}
10^{-4}
(P,R)
(R,P)
(C,P)
Total
Al Kα$_1$
a
0
20
40
60
80
100
120
E_0 (keV)

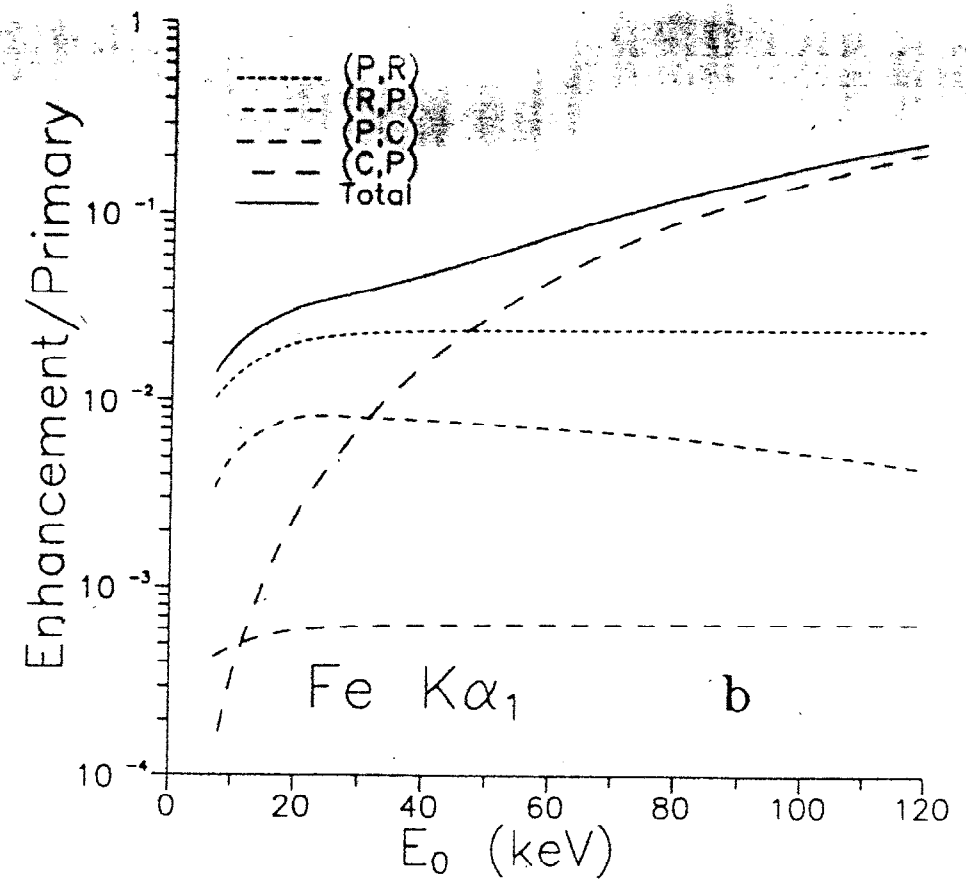
(P,R)
(R,P)
(P,C)
(C,P)
Total
Enhancement/Primary
1
10^{-1}
10^{-2}
10^{-3}
10^{-4}
0
20
40
60
80
100
120
E_0 (keV)
Fe $K\alpha_1$
b

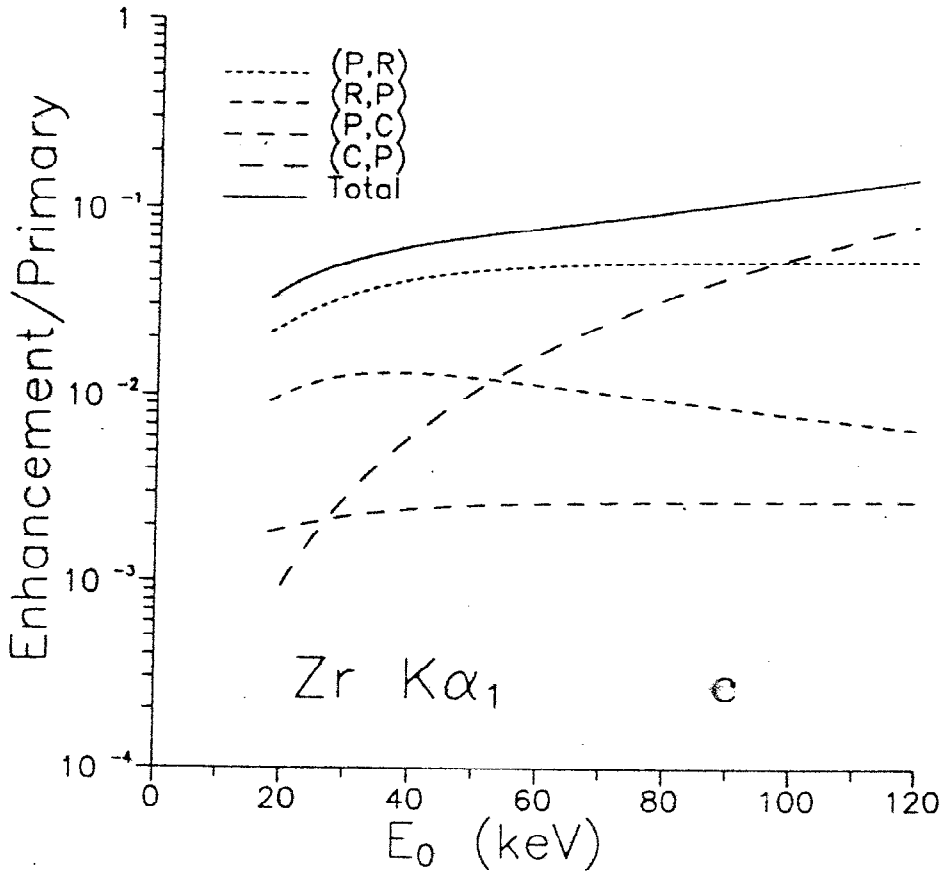
(P,R)
(R,P)
(P,C)
(C,P)
Total
Enhancement/Primary
1
10^{-1}
10^{-2}
10^{-3}
10^{-4}
0
20
40
60
80
100
120
E_0 (keV)
Zr $K\alpha_1$
c

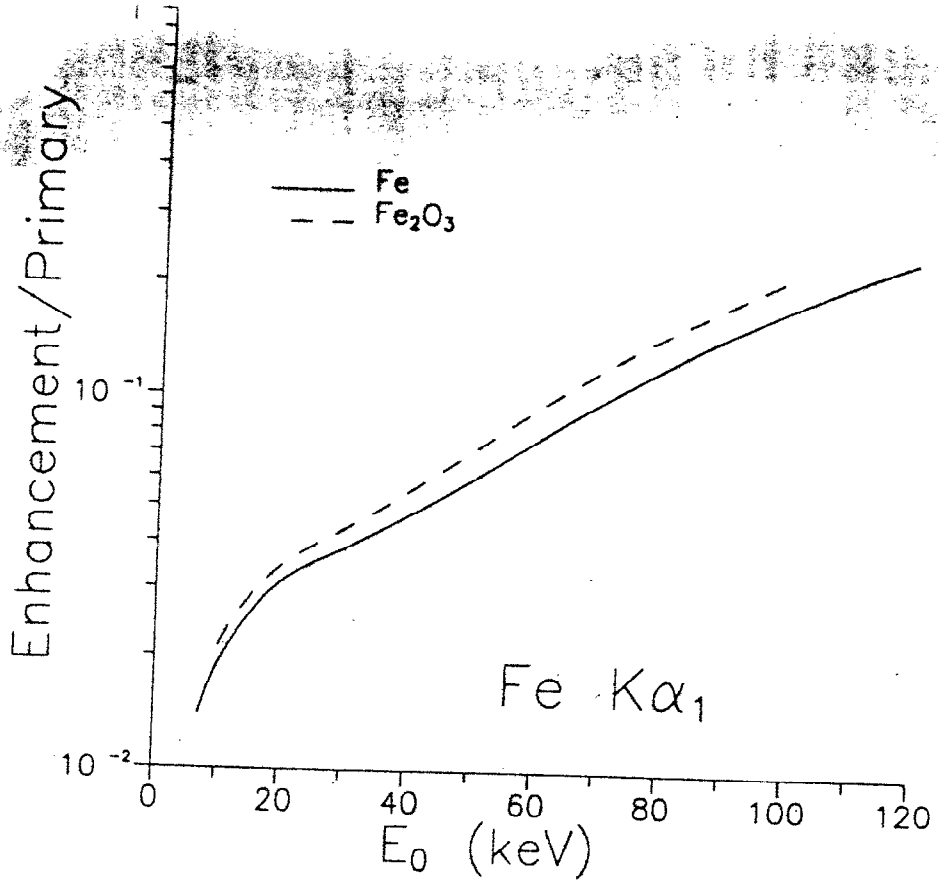
Enhancement/Primary
Fe
Fe_2O_3
10^{-1}
10^{-2}
Fe $K\alpha_1$
0
20
40
60
80
100
120
E_0 (keV)

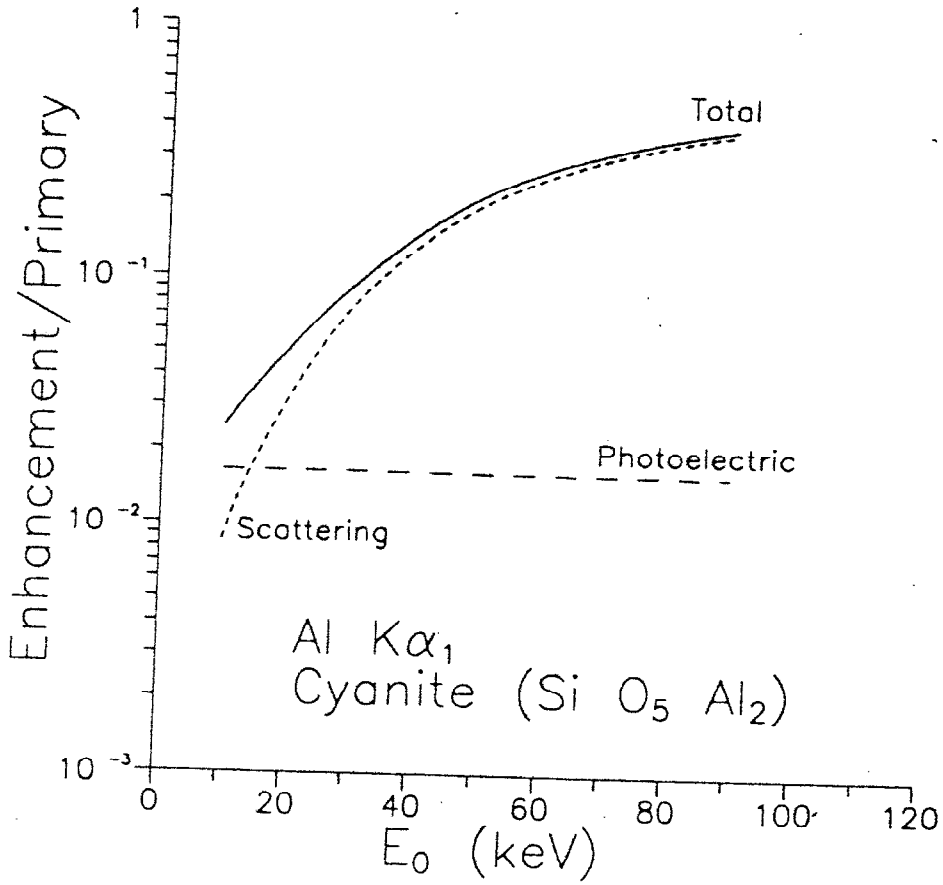
Enhancement/Primary
1
10^{-1}
10^{-2}
10^{-3}
Total
Photoelectric
Scattering
Al $K\alpha_1$
Cyanite (Si O_5 Al_2)
0
20
40
60
80
100
120
E_0 (keV)

THE CONTINUOUS SPECTRUM OF THE (P,C) CONTRIBUTION

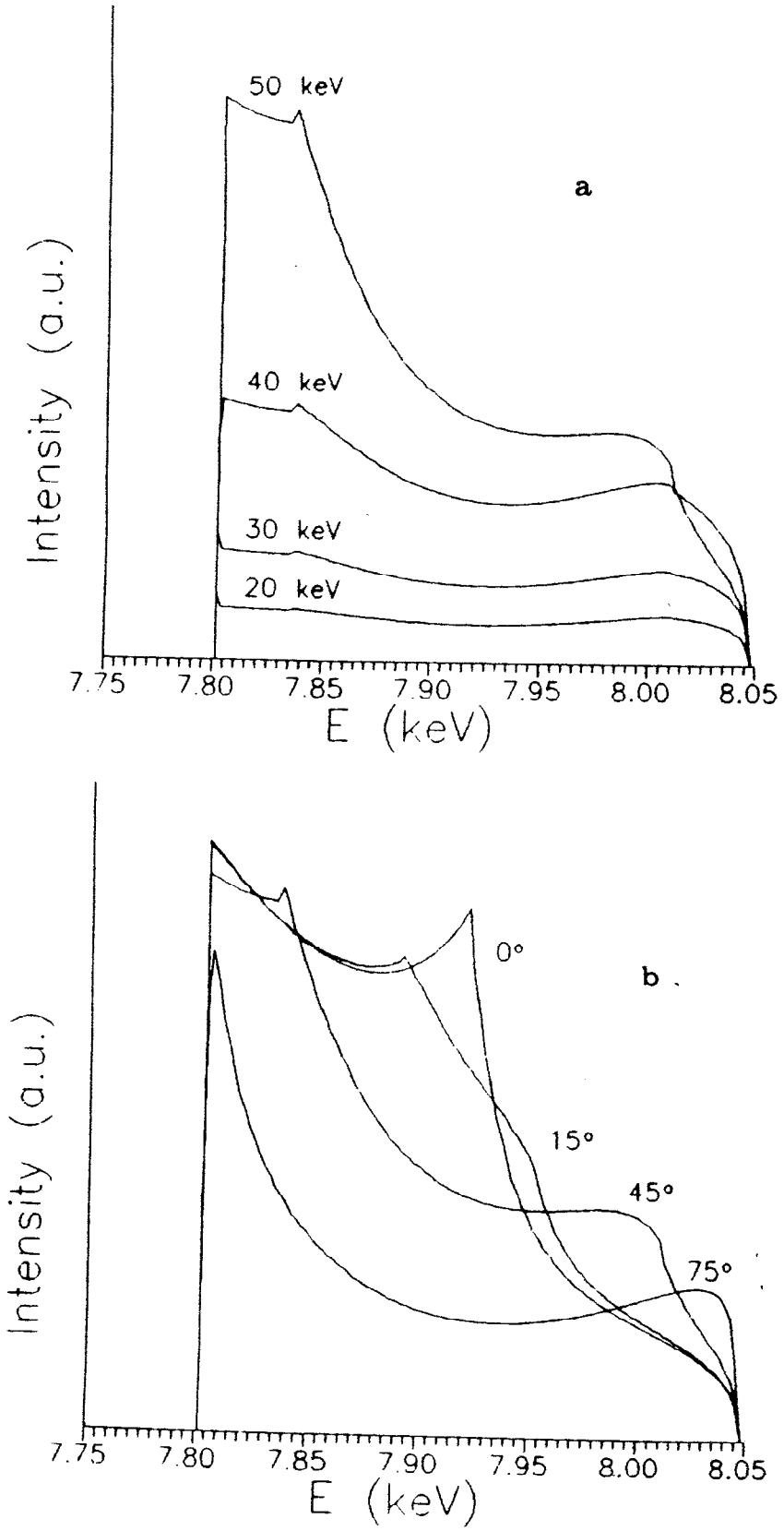

The (P,C) continuous contribution to the Cu $K\alpha_1$ line in a pure Cu sample for (a) variable excitation energy E_0 ($\vartheta_0 = 45^\circ$), and (b) variable angle of incidence ϑ_0 ($E_0 = 10$ keV).

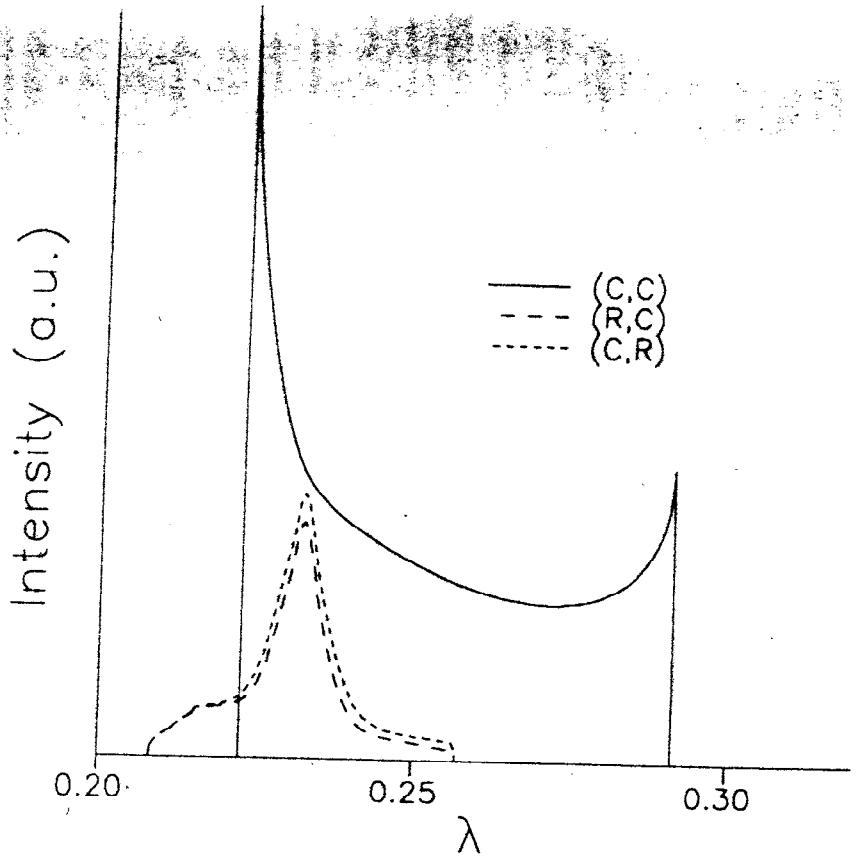
Intensity (a.u.)
(C,C)
(R,C)
(C,R)
0.20
0.25
0.30
λ

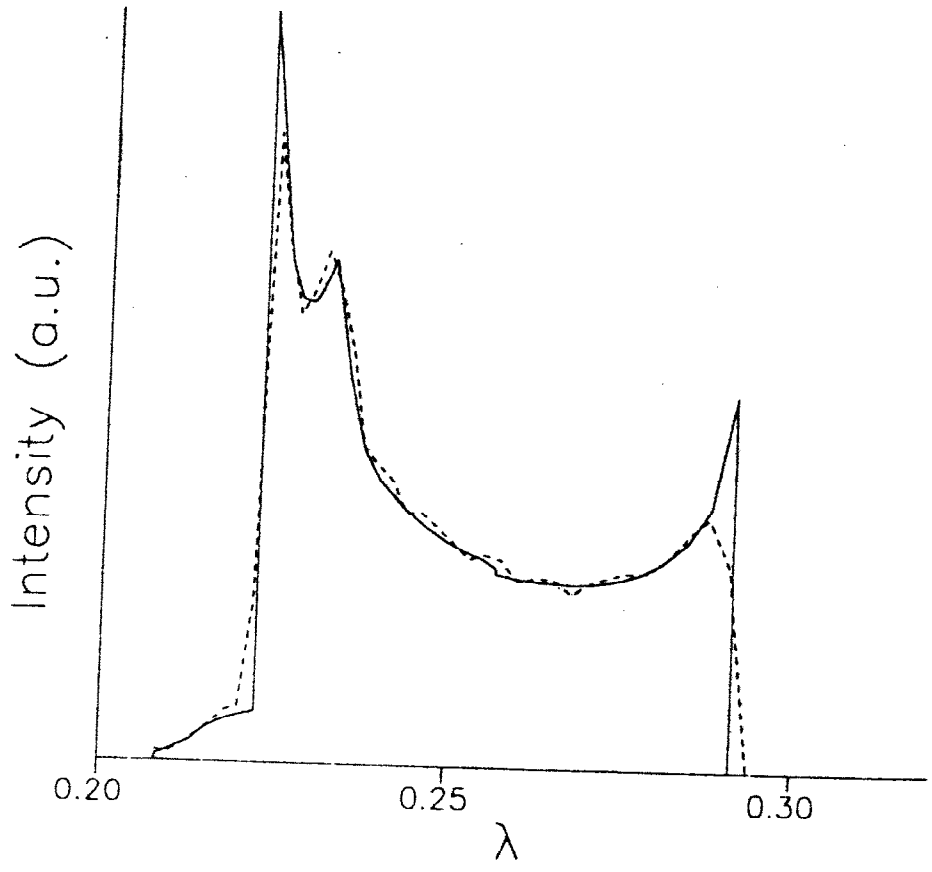
Intensity (a.u.)
0.20
0.25
0.30
λ

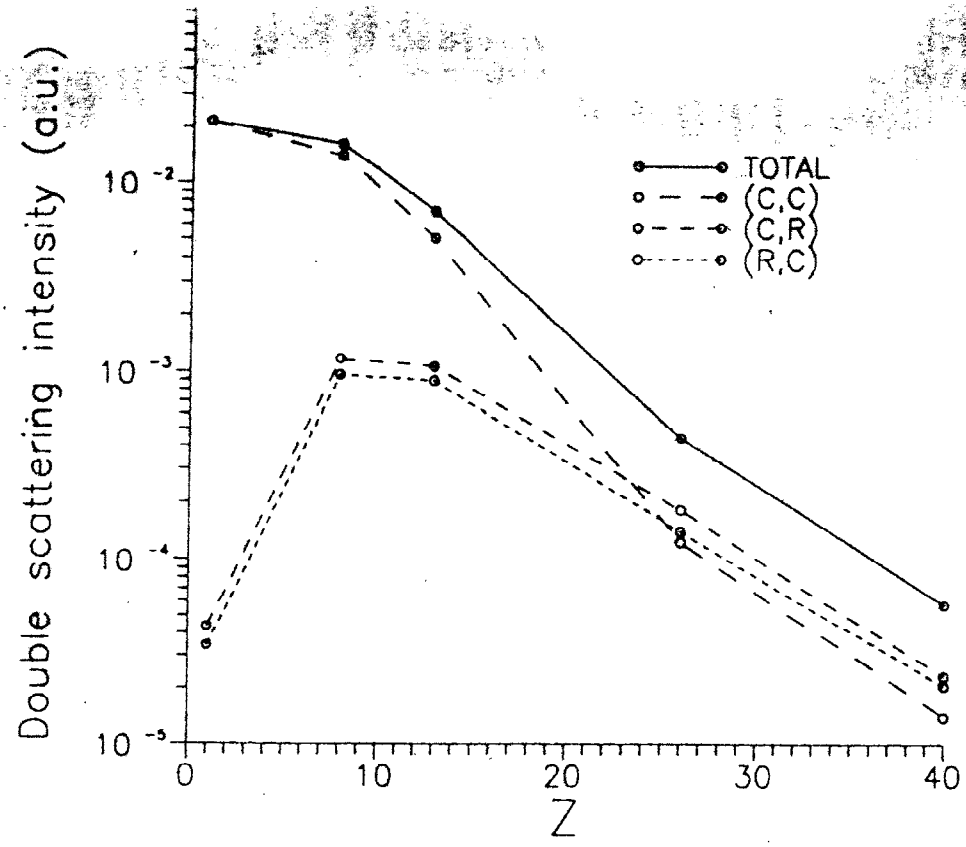
Double scattering intensity (a.u.)
10 -2
10 -3
10 -4
10 -5
0
10
20
30
40
Z
TOTAL
(C,C)
(C,R)
(R,C)

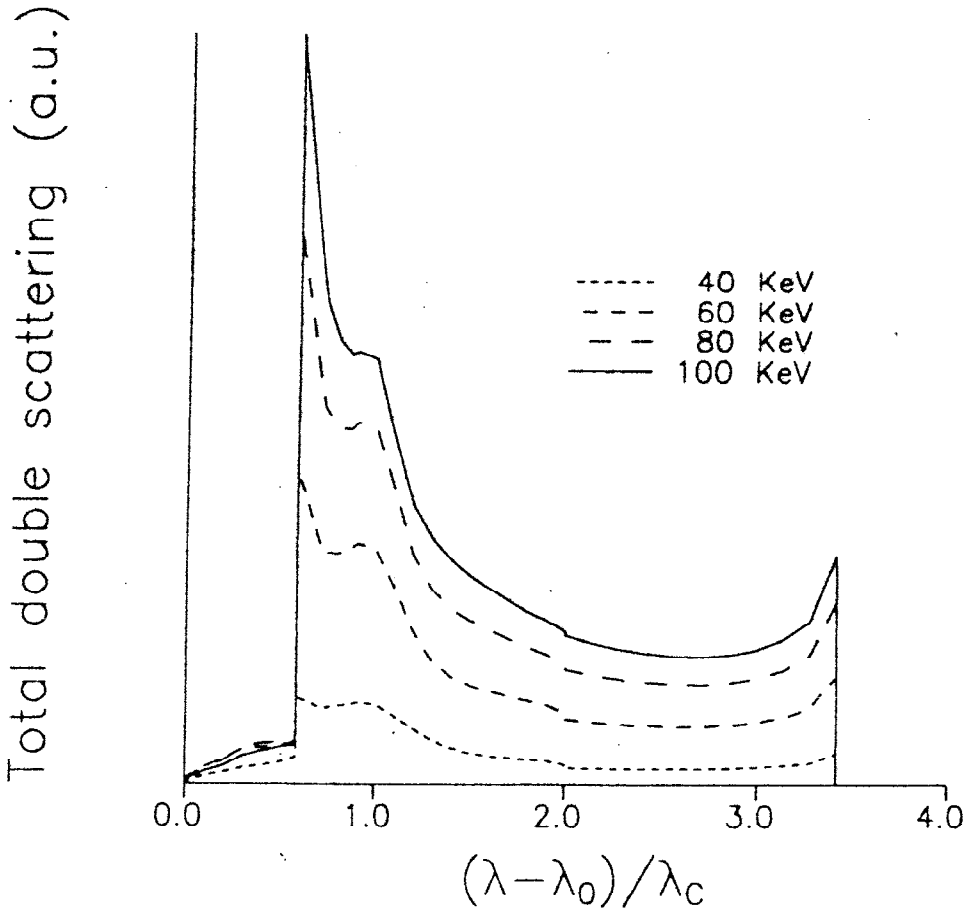
Total double scattering (a.u.)
40 KeV
60 KeV
80 KeV
100 KeV
0.0
1.0
2.0
3.0
4.0
(λ−λ0)/λc

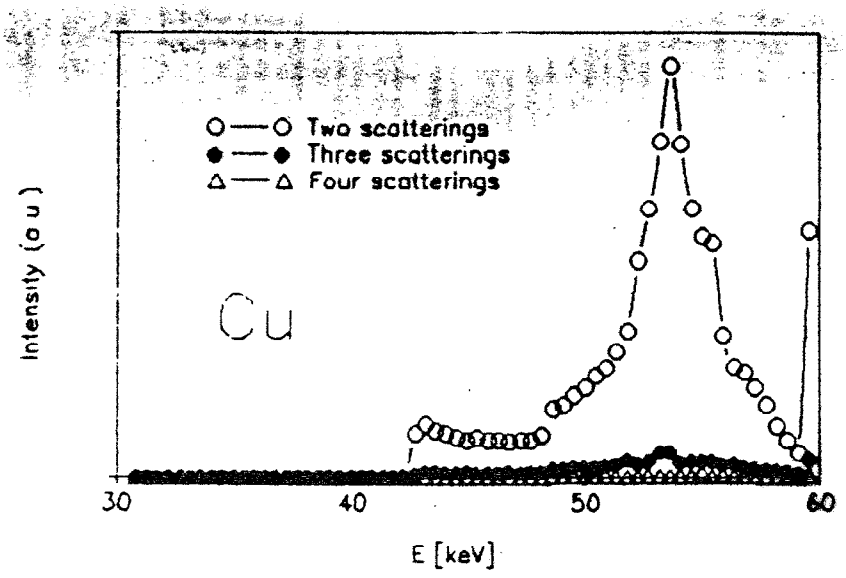
Two scatterings
Three scatterings
Four scatterings
Cu
Intensity (a u)
30
40
50
60
E [keV]

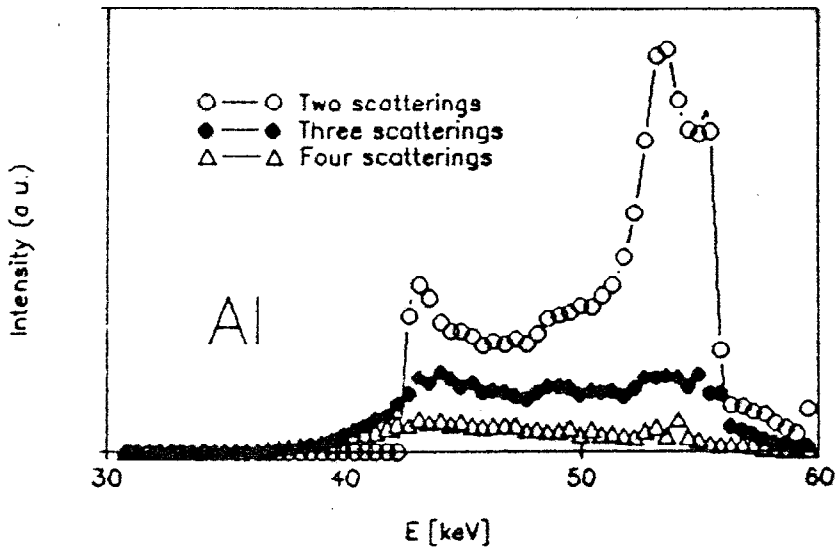
Two scatterings
Three scatterings
Four scatterings
Al
Intensity (a u.)
30
40
50
60
E [keV]

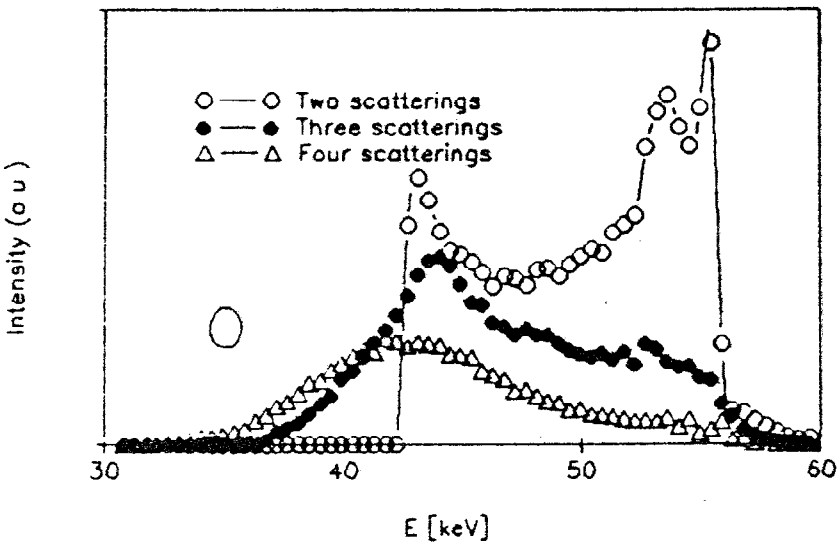
Two scatterings
Three scatterings
Four scatterings
O
Intensity (a u)
30
40
50
60
E [keV]

Detector response

$$R(E_0,E) = (1-\chi(E_0))\frac{0.9395}{FWHM(E_0)} e^{-2.773\frac{(E-E_0)^2}{FWHM^2(E_0)}} +$$

$$\chi(E_0)\frac{0.9395}{FWHM(E_0-E_{k_{Ge}})} e^{-2.773\frac{(E_0-E_{k_{Ge}}-E)^2}{FWHM^2(E_0-E_{k_{Ge}})}}$$

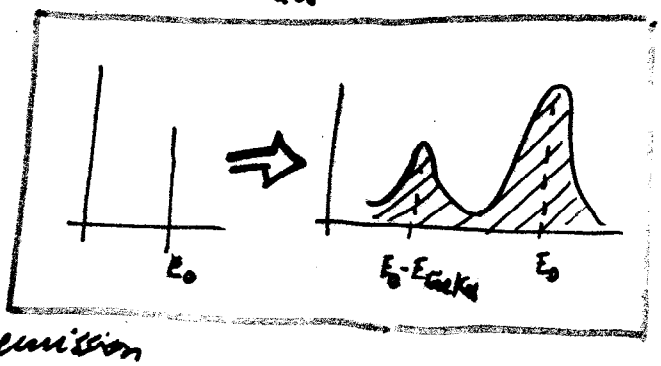

where

$\phi(E_0)$ = efficiency at energy E_0

$\chi(E_0)$ = probability of escape peak emission

$$\chi(E_0) = 0.5\,\omega_{k_{Ge}}\left(1-\frac{1}{f_{k_{Ge}}}\right)\left[1-\frac{\mu_{Ge}(Ge k_\alpha)}{\mu_{Ge}(E_0)}\ln\left(1+\frac{\mu_{Ge}(E_0)}{\mu_{Ge}(Ge k_\alpha)}\right)\right]U(E_0-E_{Ge k_\alpha})$$

FWHM(E) = full width at half maximum

$$FWHM(E) = 2.355\sqrt{(\Delta E_0)^2 + f\,\varepsilon\,E_0}$$

f ← effective Fano factor

Some properties

$$\int R(E_0,E)\,dE = 1 \qquad \text{NORMALIZATION}$$

$$\tilde{I}(E) = \int R(E',E)\,I(E')\,\phi(E')\,dE'$$

ϕ ← efficiency

Comparison with experimental data

- If data are in energy we must transform our theoretical spectrum to energy (originally in wavelength)

- We have a part of the spectrum composed of discrete lines and a part with continuum. How do the discrete lines add to the continuum?
  We know the intensity of every line, not the distribution.
  We should assign a distribution (gaussian) to each line whose FWHM is given by the natural line width. After that we have a full continuous spectrum.

- Experimental data are in MCA format so we must divide the energy range as in a MCA, and digitalize the spectrum.

- Experimental data are of detected photons so we simulate a response function of a state-of-the-art radiation detector having
  - line broadening as a function of energy
  - efficiency as a function of energy
  - escape peak creation

Computation of X-Ray spectra

CODE: SHAPE

Reference: SHAPE: a computer simulation of energy dispersive X-ray spectra.

Author(s): J.E. Fernández and M. Sumini

Description: X-ray spectrum theoretical computation taking into account multiple scattering (photon-photon) processes of photoelectric, Rayleigh and Compton effects, for any element or mixture. Results allow the identification of different chain contributions of multiple scattering, and include detector response modification.
Geometry of excitation-detection and energy of the monochromatic source are interactively defined, as much as sample composition and detector characteristics.

THE CODE

NAME	SHAPE
MODULES	SHAPE1, SHAPE2
LANGUAGE	Pascal
COMPUTER	IBM PC
REQUIREMENTS	400 KB RAM
	Numerical coprocessor (recommended)
	Parameters data base
USAGE	Interactive

SHAPE1

Evaluates the first and second order contributions of the photoelectric effect and the Rayleigh and Compton scattering.

Computes the theoretical spectrum (in wavelength) on the surface of the target.

SHAPE2

Converts the wavelength spectrum to energy.

Converts monochromatic contributions into continuous ones.

Produces an MCA discretized spectrum simulating 1024 channels.

Filters the response through a Ge solid-state detector characteristic function.

PARAMETERS DATA BASE

PARAM containing the atomic number, the chemical symbol, the atomic weight, the density and the conversion constant from barns/atom to cm^2/g.

MCMASTER containing the McMaster coefficients for the photoelectric series K, L and M, and for integrated coherent and incoherent scattering.

EDGES containing the data related to the spectral series as spectral symbol, absorption edge energy, absorption edge jump, and fluorescence yield

LINES containing the data on every single line as the spectral series to which it belongs, its spectroscopic symbol, its energy, and its line fraction.

CROMER containing the parameters for computing the coherent and the incoherent scattering functions.

SHAPE'S FILE OUTPUT

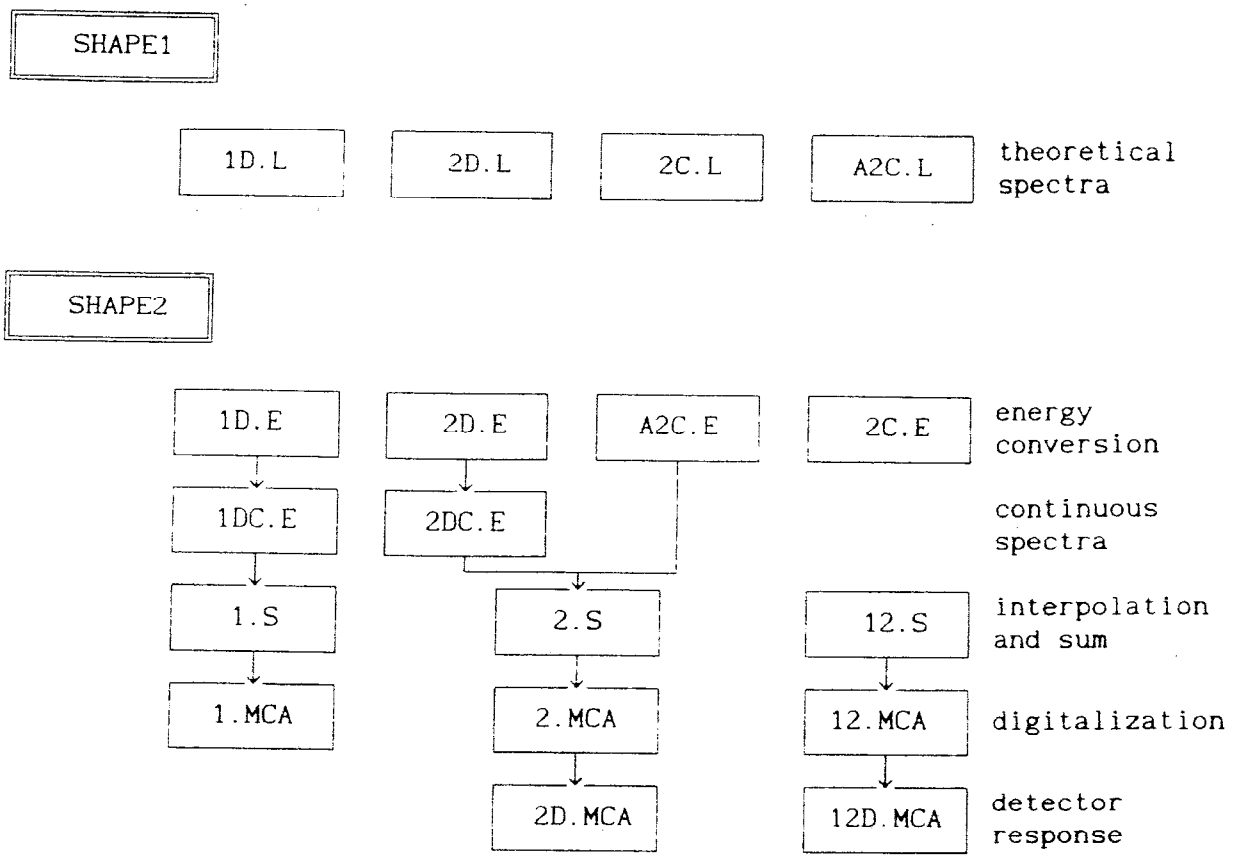

File output of the two steps of SHAPE for the different stages of computation.

TEST PROBLEM

SAMPLE	Fe (75%) - Ni (25%)
EXCITATION ENERGY	10 keV
GEOMETRY (45/135/0)	Polar incidence 45°
	Polar take-off 45°
	Azimuthal angle 0°
COMMENTS	XRF characteristic lines showing the total and second order contributions.

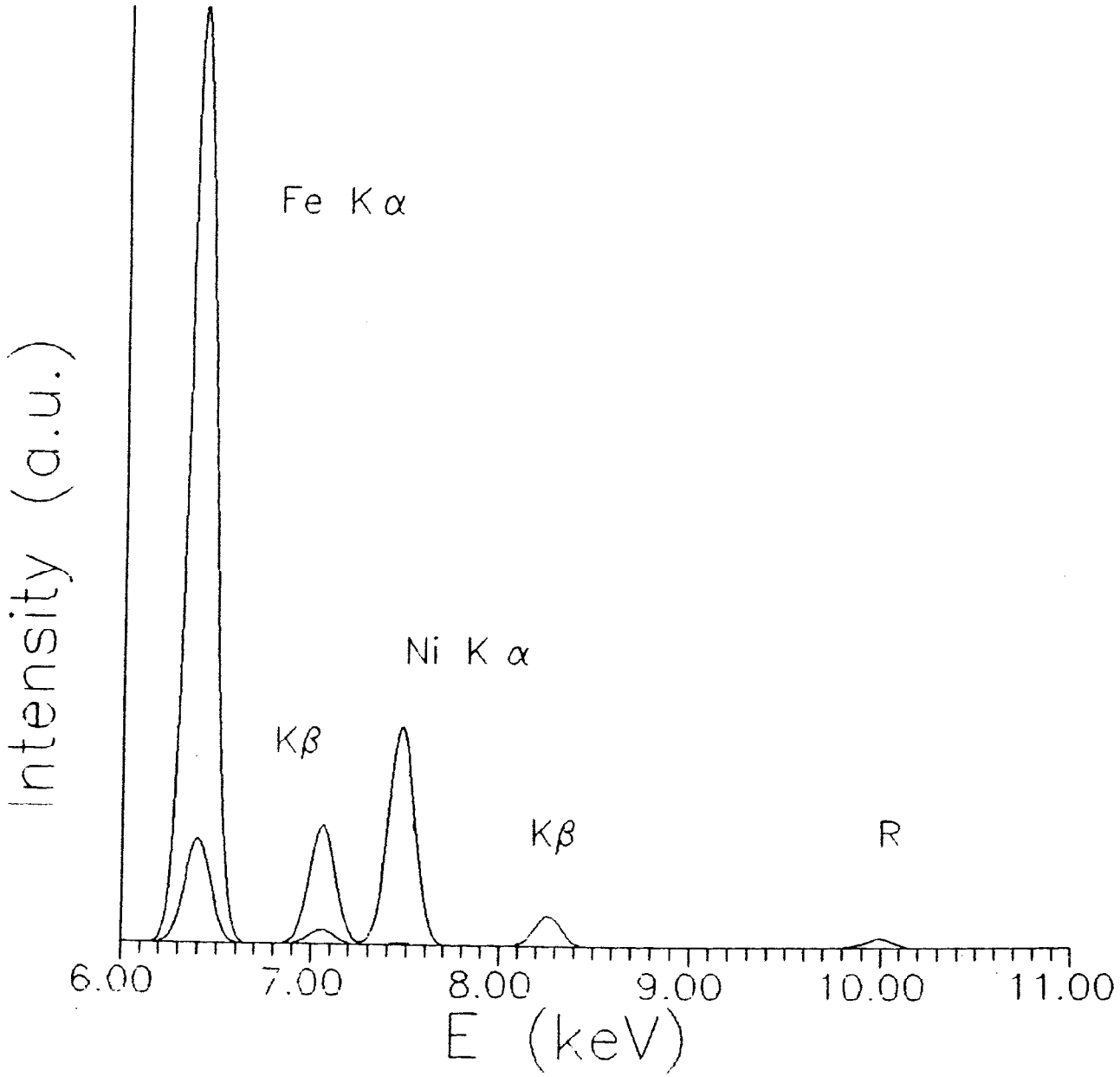

TEST PROBLEM

SAMPLE	SiO_2 (90%) - Fe_2O_3 (10%)
EXCITATION ENERGY	10 keV
GEOMETRY (45/135/0)	Polar incidence 45°
	Polar take-off 45°
	Azimuthal angle 0°
COMMENTS	Fe XRF characteristic lines showing the enhancement due to scattering

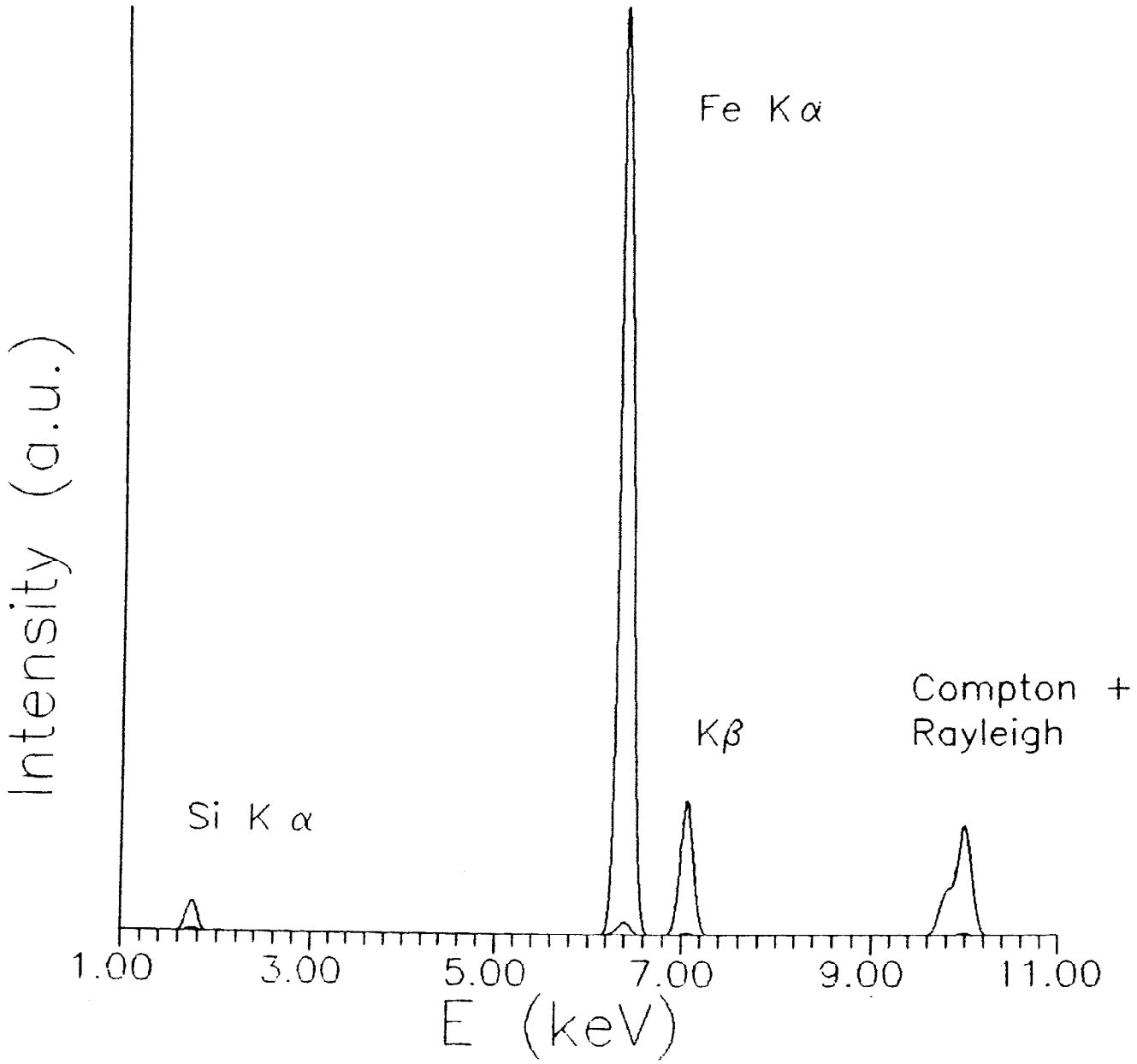

TEST PROBLEM

SAMPLE	SiO_2 (90%) - Fe_2O_3 (10%)
EXCITATION ENERGY	50 keV
GEOMETRY (45/135/0)	Polar incidence 45°
	Polar take-off 45°
	Azimuthal angle 0°
COMMENTS	Scattering spectrum showing the importance of the second order contribution.

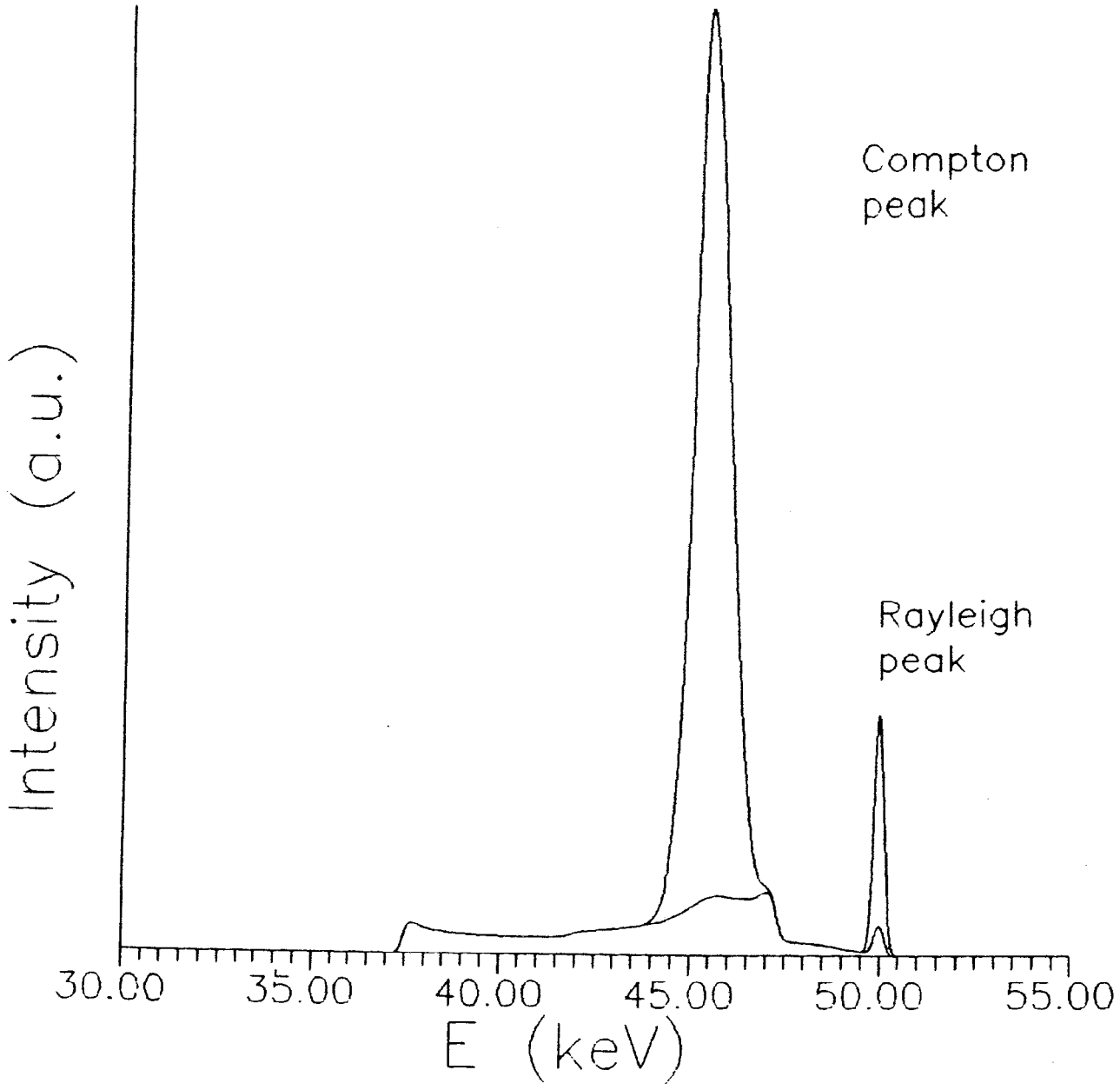

TEST PROBLEM

SAMPLE	H_2O
EXCITATION ENERGY	59.54 keV (^{241}Am)
GEOMETRY (45/135/0)	Polar incidence 45°
	Polar take-off 45°
	Azimuthal angle 0°
COMMENTS	Comparison with experimental data obtained with a 5mm thick pure Ge detector (same as simulated by SHAPE).